Virchows Archiv (2019) 474:569–575
https://doi.org/10.1007/s00428-019-02535-7

ORIGINAL ARTICLE

Clinicopathological characteristics associated with necrosis in pulmonary metastases from colorectal cancer

Jun Suzuki[1,2,3] · Motohiro Kojima[1] · Keiju Aokage[2] · Takashi Sakai[1,2] · Hiroshi Nakamura[1,3] · Yuuki Ohara[1,4] · Kenta Tane[2] · Tomohiro Miyoshi[2] · Masato Sugano[4] · Satoshi Fujii[1] · Takeshi Kuwata[4] · Atsushi Ochiai[5] · Masaaki Ito[6] · Kenji Suzuki[3] · Masahiro Tsuboi[2] · Genichiro Ishii[1]

Received: 2 November 2018 / Revised: 23 January 2019 / Accepted: 28 January 2019 / Published online: 14 February 2019

Abstract

Metastatic lung cancers from the colon and rectum (MLCR) frequently have necrotic components. The aim of this study is to elucidate clinicopathological factors associated with the amount of necrosis in MLCR. Ninety patients who underwent the first pulmonary metastasectomy for MLCR with a tumor diameter ≦ 3.0 cm and without chemotherapy were enrolled in this study. Analyzing digitally scanned pathological slides, we calculated the necrosis percentage (NP, the necrosis area divided by the tumor area). The relationship between NP and clinicopathological factors was analyzed. Moreover, to determine whether NP was affected by tissue hypoxia, vascularization, or tumor cell proliferation, tissues were analyzed by immunohistochemical staining using carbonic anhydrase IX (CAIX), CD34 antibodies, and Ki-67 antibodies, respectively. Median tumor area and NP were 0.69 cm^2 (0.11–3.01) and 13.1% (0–71.6), respectively. Although NP was not associated with the tumor area, it was significantly higher in the patients with a positive smoking history (8.14% vs 17.1%, $p = 0.045$). Other clinicopathological factors were not correlated with NP. Immunohistochemical analysis revealed that CA IX expression on tumor cells, CD34 micro-vessel density, CD34 micro-vessel area, and Ki-67 index were not significantly associated with NP. NP in the primary site was not associated with NP in the pulmonary metastasis. NP was not determined by tumor size, tissue hypoxia, vascularization, or tumor cell proliferation. Positive correlation of NP with smoking history suggests a unique lung microenvironment in smokers which makes necrosis of MLCR more likely to occur.

Keywords Colorectal cancer · Pulmonary metastasis · Pathology · Necrosis

This article is part of the Topical Collection on *Quality in Pathology*

Electronic supplementary material The online version of this article (https://doi.org/10.1007/s00428-019-02535-7) contains supplementary material, which is available to authorized users.

✉ Genichiro Ishii
gishii@east.ncc.go.jp

[1] Division of Pathology, Exploratory Oncology Research and Clinical Trial Center, National Cancer Center 6-5-1, Kashiwanoha, Kashiwa, Chiba 277-8577, Japan

[2] Department of Thoracic Surgery, National Cancer Center Hospital East, Chiba, Japan

[3] Department of General Thoracic Surgery, Juntendo University School of Medicine, Tokyo, Japan

[4] Department of Pathology and Clinical Laboratories, National Cancer Center Hospital East, Chiba, Japan

[5] Exploratory Oncology Research and Clinical Trial Center, National Cancer Center, Chiba, Japan

[6] Department of Colorectal Surgery, National Cancer Center Hospital East, Kashiwa, Chiba, Japan

Introduction

Colorectal cancer is one of the most common cancers and causes of cancer deaths worldwide [1]. The most common extra-abdominal organ site of metastases of colorectal cancer is the lung, involved in 10–25% of all patients with colorectal cancer [2, 3].

The characteristic pathological findings of metastatic lung cancer from the colon and rectum (MLCR) include glands lined by pseudostratified columnar cells and extensive necrosis with karyorrhectic debris, also known as dirty necrosis [4]. The presence of dirty necrosis in malignant pulmonary tumors suggests a colorectal origin [5].

Generally, tumor necrosis results from chronic hypoxia due to rapid tumor growth. This could be caused by the rapidly proliferating tumor obstructing the focal large vessels or microvasculature [6, 7]. Väyrynen et al. investigated the causes of necrosis in colorectal cancer by examining cell proliferation (Ki-67 index) and neovascularization (microvessel density),

both of which were determined to be negative [8]. Otherwise, there have been few studies investigating the clinicopathological factors associated with necrosis in colorectal cancer as well as in MLCR. Therefore, it needs to be clarified whether tumor size, tissue hypoxia, neovascularization, or cell proliferation is correlated with the amount of necrosis in MLCR. Hence, this study aims to investigate clinicopathological characteristics that contribute to the amount of necrosis in MLCR.

Patients and methods

Case selection

We investigated a total of 168 pulmonary metastasectomy cases for MLCR with tumor diameters no less than 3.0 cm at our institution between 2013 and 2017. Among them, 52 cases were excluded because they were not the first metastasectomy cases. Two cases were excluded because of another advanced active cancer. Furthermore, 24 cases in which chemotherapy had been conducted for MLCR before metastasectomy were also excluded. The remaining 90 patients were included in this study.

For each patient, the following demographic and clinicopathological factors were collected from medical records: age, sex, smoking status, location of the primary tumor, preoperative chemotherapy history, synchronous/metachronous metastases, single/multiple metastases, and tumor diameter. Synchronous lung metastasis had to be diagnosed during the diagnostic work-up or within 3 months following the diagnosis of colorectal cancer. All specimens were collected after obtaining comprehensive written informed consent from the patients. This study was approved by the Institutional Review Board of the National Cancer Center (IRB number 2018-030).

Patient follow-up

All patients were followed up at 3 to 6-month intervals after surgery. The follow-up evaluation included a history taking, physical examination, chest radiography, and blood examination. Patients who were consulted from the outside hospitals were referred back to the original hospitals after 1 to 2-year follow-up at our hospital. Computed tomography was performed at the physicians' discretion.

Histopathological evaluation

The pathological factors were evaluated by two pathologists (J.S and G.I). Tissues were fixed in neutral buffered 10% formalin solution. The hematoxylin and eosin (H&E) slides of the maximum plane of the tumor were selected. In patients with multiple metastases, the largest lesion was examined. These slides were digitally scanned and analyzed using a Hamamatsu Nanozoomer scanner (Hamamatsu NDP.view2) to calculate the tumor area (TA), necrosis area, and the necrosis percentage (NP, necrosis area divided by TA). There were two types of necrosis in MRCL: multiple small necroses and single massive necrosis (Fig. 1). The TA and the necrosis area were measured by circumscribing the whole TA and the necrosis area on the software (Supplementary Fig. 1A). In the case of multiple necroses, we included as many necrosis areas as possible (Supplementary Fig. 1B).

Immunohistochemistry

All tumor tissues used in this immunohistochemical analysis were from routinely formalin-fixed pathological samples taken from resected lung specimens. One block containing the most extensive tumor component was selected from each specimen following a review of the H&E-stained slides. Sections measuring 4 m were cut from the paraffin blocks and mounted on salinized slides. The sections were deparaffinized in xylene, dehydrated in a graded ethanol series, and then immersed in methanol with 0.3% hydrogen peroxide for 15 min to inhibit endogenous peroxidase activity. After being washed with distilled water, the sections were placed in Retrieval Solution High pH (DakoCytomation, Carpinteria, CA, USA). For antigen retrieval, the slides were heated twice at 95 °C for 20 min in a microwave oven (H2800 Microwave Processor, Energy Beam Sciences Inc.) and then cooled for 1 h at room temperature. The slides were washed three times in phosphate-buffered saline (PBS). Nonspecific binding was then blocked by pre-incubation with 2% normal swine serum in PBS (blocking buffer) for 60 min at room temperature. Individual slides were next incubated overnight at 4 °C with anti-human carbonic anhydrase IX, anti-human CD34, and anti-human Ki-67 antigen in the blocking buffer. The slides were washed three times with PBS and then incubated with EnVision™ (Dako, Denmark) for 1 h at room temperature. After extensive washing with PBS, the color reaction was developed in 2% 3,3′-diaminobenzidine in 50 mM Tris-buffer (pH 7.6) containing 0.3% hydrogen peroxidase for 10 min. The sections were finally counterstained with Meyer's hematoxylin, dehydrated, and mounted. Supplementary Table 1 summarizes the details of antibodies used in this study.

Two investigators (J.S. and G.I.) independently evaluated the staining results of CAIX. The expression of CAIX on tumor cells was measured as the proportion of positive tumor cells to total tumor cells, yielding a range of 0–100%. For CD34 microvessel density, CD34 microvessel area, and Ki-67 index, analysis was assisted by the ImageScope software program (Leica Microsystems, Wetziar, Germany, Supplementary Fig. 2). The vascular hot spot, or the area of the tumor containing many CD34 positive vessels, was detected by scanning the section at × 100 magnification

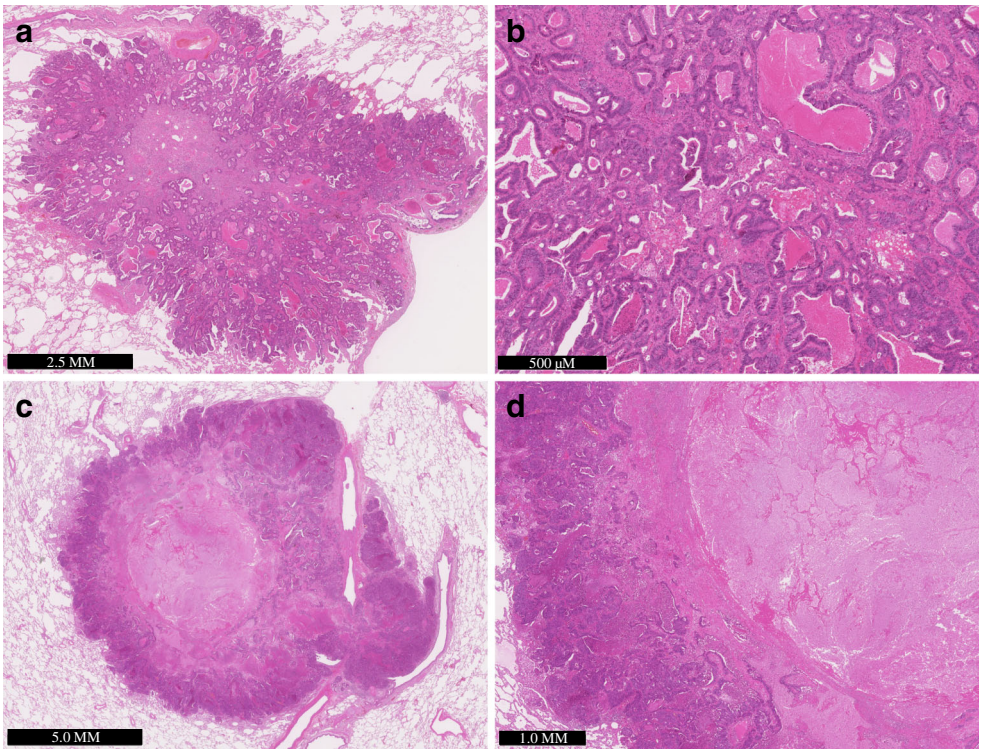

Fig. 1 The MRCL lesions with multiple small necroses (lower magnification (**a**), higher magnification (**b**)) and single massive necrosis (lower magnification (**c**), higher magnification (**d**))

(Supplementary Fig. 2A). Ten different hot spots were chosen. In each of those fields, the numbers of microvessels positive for CD34 per 0.25 mm^2 were counted (Supplementary Fig. 2B). The average of the ten areas was calculated as mean microvessel density (MVD, number of vessels per mm^2). In addition to the number of vessels, we calculated the average area of the CD34-positive microvessels per square micrometer as microvessel area (MVA), which reflects both number and lumen area of the microvessels (Supplementary Fig. 2B) [9]. Ki-67 index was determined by the mean proportion of tumor cell nuclei positive for Ki-67 in three different hot spots (Supplementary Fig. 2C).

Table 1 Patient characteristics

$N = 90$		Necrosis percentage (%)	p value
Median age	67 (35–85)	9.73 (0–71.6)	0.81
≦ 65	37 (41.1%)	14.1 (0–65.3)	
< 65	53 (58.9%)		
Sex	63 (70.0%)	14.1 (0–71.6)	0.12
Male	27 (30.0%)	8.2 (0–65.3)	
Female			
Smoking status	31 (34.4%)	8.14 (0–65.3)	0.045
Never/light	59 (65.6%)	17.1 (0–71.6)	
Positive			
Timing of metastasis	12 (13.3%)	14.9 (1.34–64.6)	0.94
Synchronous	78 (66.7%)	12.6 (0–71.6)	
Metachronous			
Number of metastatic lesions	77 (85.6%)	13.8 (0–71.6)	0.81
Single	13 (14.4%)	12.7 (0–44.5)	
Multiple			
Location of the primary tumor	9 (10.0%)	23.5 (0–40.8)	0.90
Right-sided colon	24 (26.7%)	14.3 (0–71.6)	
Left-sided colon	36 (40.0%)	13.3 (0–64.1)	
Upper rectum	21 (23.3%)	7.2 (0–65.3)	
Lower rectum			

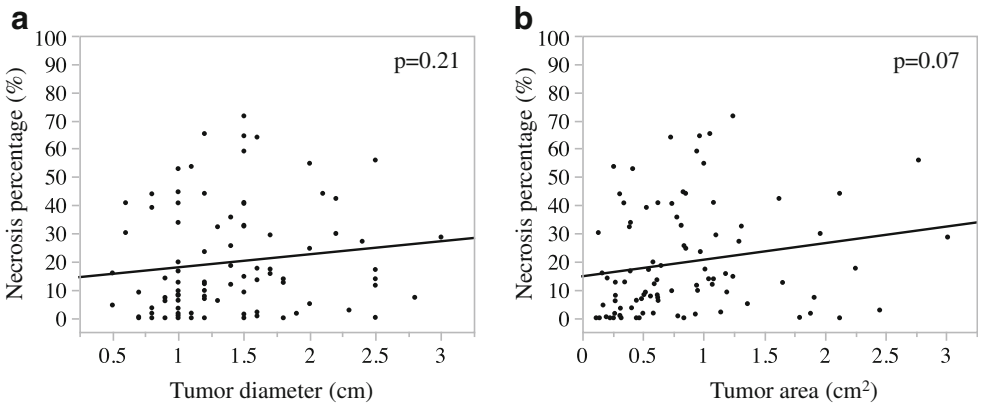

Fig. 2 The scatter plots showing the relationship between necrosis percentage and tumor diameter (**a**) or TA (**b**)

Statistical analysis

Comparisons between the necrosis percentage and clinicopathological factors and immunohistochemistry factors were analyzed using a chi-square test for proportions and analysis of variance (ANOVA) test for continuous variables as appropriate. Calculation of the recurrence-free survival (RFS) and the overall survival (OS) was performed using the Kaplan–Meier method, and compared using the log-rank test. All statistical analyses were performed using JMP® Version 12 (SAS Institute Inc., Cary, NC).

Results

Patient and pathological characteristics

Of the 90 patients, 63 (70%) were men. Median (range) age was 67.0 (35–85). Thirty-one (34.4%) were non-smokers or light smokers (smoking index less than 50). Synchronous metastasis and multiple metastases were seen in 12 (13.3%) and 13 (14.4%) patients, respectively. The upper rectum was the most common site of the primary CRC location and was seen in 36 (40.0%) patients (Table 1).

Necrosis percentage and its relation to the clinical and pathological factors

The median (range) of tumor diameter, TA, and NP were 1.3 cm (0.5–3.0), 0.69 cm^2 (0.11–3.01), and 13.1% (0–71.6), respectively (Supplementary Table 2). Both tumor diameter and TA were not significantly correlated to NP ($p = 0.21$ and $p = 0.07$, respectively, Fig. 2). NP was significantly higher in the patients with positive smoking history compared to never/light smokers (8.1% [0–65.3] vs 17.1% [0–71.6], $p = 0.045$). Other clinical factors did not affect NP.

Necrosis percentage and the survival analysis

The survival analysis was conducted for 112 patients who achieved complete resection. Median follow-up period after metastasectomy was 24.5 months (range 0.8–67.7). When the patients were divided into two groups based on the median value of necrosis percentage (low necrosis vs high necrosis, cutoff value = 13.5%), there was no significant difference in the RFS between the two groups (median RFS, low necrosis 5.9 months vs high necrosis 12.6 months; $p = 0.31$). The OS did not differ between the two groups (median OS, low necrosis 18.5 months vs high necrosis 28.4 months; $p = 0.14$). Kaplan–Meier curves for the RFS and the OS are shown in Supplementary Fig. 5.

Immunohistochemical analysis

Median Ki-67 index, CAIX positive percentage, CD34 MVD, and MVA were 37.2% (5.2–71.9), 15% (0–70), 65.4 per mm^2 (21.6–190), and 793.2 per μm^2 (308.4–2238.3). None of these factors was significantly associated with NP ($p = 0.72$, $p = 0.56$, $p = 0.20$, and $p = 0.09$, respectively, Fig. 3D, E, F, and G).

Comparison of NP between the primary site and the metastatic site

Of the 90 cases, pathological slides of the primary site were available for 35 cases. We evaluated NP in the primary site in 35 cases in the same way as the metastatic site. The background of these patients was summarized in Supplementary Table 3. The median NP was 0.027% (0–16.3). Although NP was not significantly correlated with tumor diameter ($p = 0.07$, Supplementary Fig. 3A), it was significantly associated with the TA ($p = 0.0001$, Supplementary Fig. 3B). There are some cases in which a negligible amount of necrosis was present in the primary site (Fig. 4A), whereas massive necrosis was seen in the pulmonary metastasis (Fig. 4B). However, when

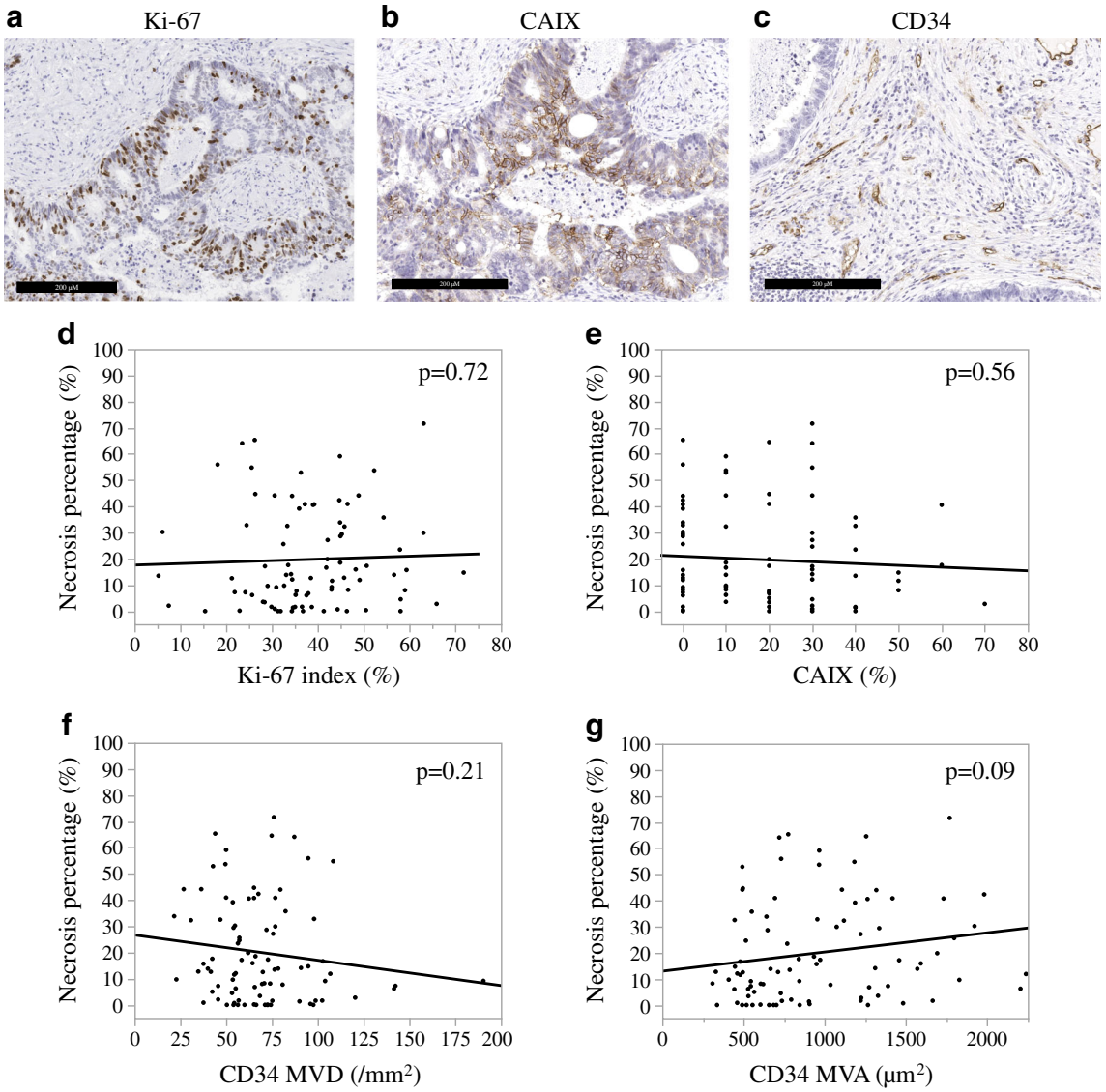

Fig. 3 The immunohistochemical staining of Ki-67 (**a**), carbonic anhydrase IX (CAIX, **b**), and CD34 (**c**) to evaluate cell proliferation (Ki-67 index) tissue hypoxia, vascularization (microvessel density [MVD; number of microvessels per mm^2], and microvessel area [MVA; area of microvessels per μm^2]). Scatter plot analysis revealed none of these were correlated to the necrosis percentage (**d**, **e**, **f**, and **g**)

investigating the relationship between NP in the primary site and NP in the matched metastatic site, there was no significant correlation ($p = 0.88$, Fig. 4C).

Discussion

This is the first study that evaluated the necrosis percentage in MLCR and analyzed its association with clinicopathological factors, tumor size, tissue hypoxia, vascularization, cell proliferation, and necrosis in the primary site. Our results revealed that positive smoking history was significantly correlated to NP in MLCR, whereas other clinicopathological factors were not. Biological features of MLCR investigated by immunohistochemistry revealed no significant relationship with NP. The necrosis percentage did not affect the prognosis of MLCR.

There have been other studies investigating necrosis in primary colorectal cancer. Väyrynen et al. measured NP accurately by analyzing virtual slides, which we adopted in our study, and reported that the median NP was 10% [8]. They also found that the NP was higher in advanced TMN stages; however, it was not associated with preoperative chemotherapy, tumor growth (Ki-67 index), or neovascularization (MVD) [8]. Other studies reported that mild to moderate necrosis was seen in about 80% of all primary site tumors, and tumor necrosis was higher in the larger tumors [10, 11], which was consistent with our results. Our current study revealed that MLCR, when compared to the primary site, was not determined by the tumor size.

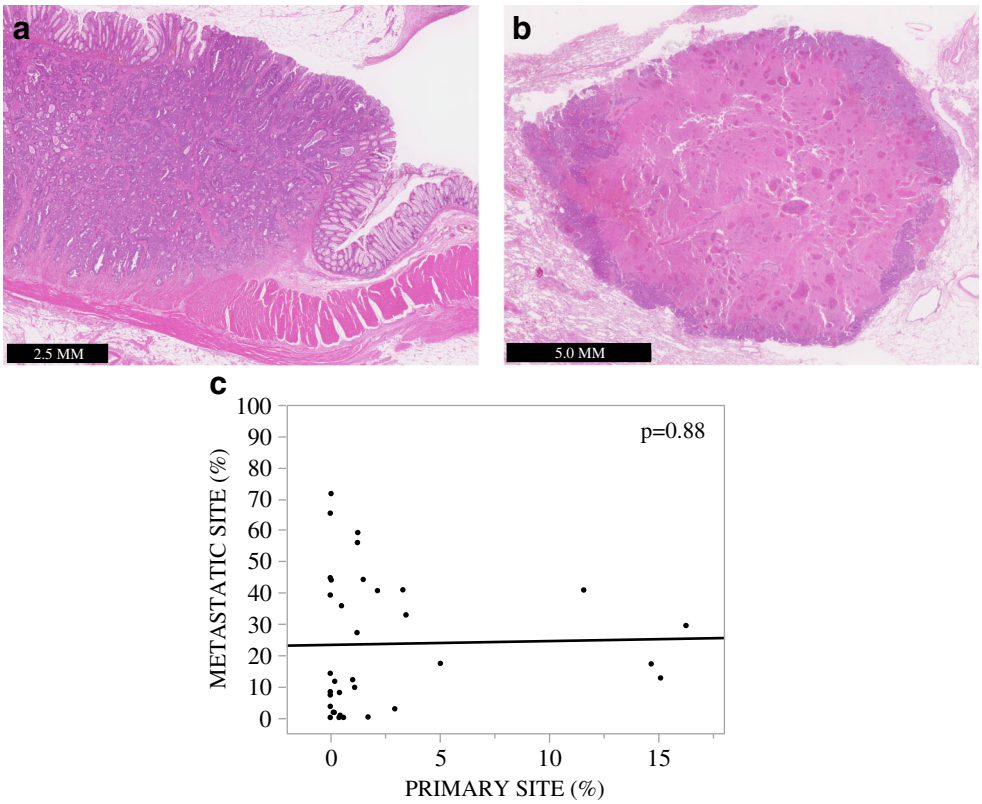

Fig. 4 Example of the cases in which a negligible amount of necrosis was present in the primary site (**a**) while massive necrosis was seen in the pulmonary metastasis (**b**). There was no correlation between the necrosis percentage in the primary site and the metastatic site (**c**)

In some cancers including colorectal cancer, extensive necrosis in the primary site has been reported to be associated with worse prognosis [8, 10–13]. Our results revealed that there was no significant difference in the prognosis between patients with high and low necrosis percentage. However, this requires cautious interpretation, because our follow-up data might be immature; 47 (42%) patients were consulted back to the original hospital after 1 to 2 years after surgery and the follow-up information thereafter was not collected in most of the cases.

Preoperative chemotherapy reportedly affects necrosis in liver metastases. Some reports suggest that abundant necrosis was seen in patients who had preoperative chemotherapy, especially in those who had been treated with bevacizumab [14–17]. In our data, NP of the patient who had preoperative chemotherapy for MRLC did not differ compared to the patient who did not (13.3% [0–58.7] vs 13.1% [0–71.6], $p = 0.27$, Supplementary Fig. 4). Although the chemotherapy regimens used in our patients varied, our study suggested that preoperative chemotherapy was not associated with NP.

It remains unclear what contributes to the development of necrosis in MLCR. Another possibility could be the tissue microenvironment of the lung, which is suggested by the positive association between smoking history and NP found in our results. According to the "seed and soil" hypothesis, the tumor cells (seed) need a hospitable microenvironment (soil) to colonize distant organs [18]. Some research suggests that smoking induces elevated inflammatory cytokines such as IL-8 and IL-1, causing inflammatory changes in the lung microenvironment [19, 20]. Inflammatory processes may establish a premetastatic niche for MLCR [21, 22]. Furthermore, smoking is reportedly associated with increased risk of pulmonary metastasis in colorectal cancer [23]. An inflammatory background might also play some role in creating the unique microenvironment for MLCR that promotes necrosis.

In conclusion, NP in MLCR was not affected by tumor size, tissue hypoxia, vascularization, or cell proliferation. The significant correlation between NP and smoking history suggests that MLCR itself has unique biological features that promote necrosis in the lung microenvironment of smokers. Further research is necessary to clarify the mechanisms of necrosis in MLCR.

Author contributions JS and GI contributed to the design and organization and conducted the study and wrote the manuscript. TS and HN helped in the immunohistochemical process and created the pathological database. MK, YO, MS, MF, TK, AO, and KS advised the direction of study and the interpretation of the data. KA, KT, TM, MI, and MT contributed to provide surgical samples and clinical data. All the authors reviewed and accepted the manuscript.

Funding This work was supported in part by JSPS KAKENHI (16H05311).

Compliance with ethical standards

Conflict of interest The authors declare that they have no conflict of interest.

Publisher's note Springer Nature remains neutral with regard to jurisdictional claims in published maps and institutional affiliations.

References

1. GLOBOCAN, International Agencyfor Research on Cancer, WHO. Cancer today: estimated number of incident cases, both sexes, Worldwide (Top 10 Cancer Sites) in 2012. 2018
2. Inoue M, Ohta M, Iuchi K, Matsumura A, Ideguchi K, Yasumitsu T, Nakagawa K, Fukuhara K, Maeda H, Takeda S, Minami M, Ohno Y, Matsuda H, Thoracic Surgery Study Group of Osaka University (2004) Benefits of surgery for patients with pulmonary metastases from colorectal carcinoma. Ann Thorac Surg 78(1):238–244
3. Rama N, Monteiro A, Bernardo JE, Eugénio L, Antunes MJ (2009) Lung metastases from colorectal cancer: surgical resection and prognostic factors. Eur J Cardiothorac Surg 35(3):444–449
4. Marchevsky AM, Gupta R, Balzer B (2010) Diagnosis of metastatic neoplasms: a clinicopathologic and morphologic approach. Arch Pathol Lab Med 134(2):194–206
5. Flint A, Lloyd RV (1992) Pulmonary metastases of colonic carcinoma. Distinction from pulmonary adenocarcinoma. Arch Pathol Lab Med 116(1):39–42
6. Caruso RA et al (2014) Mechanisms of coagulative necrosis in malignant epithelial tumors (review). Oncol Lett 8(4):1397–1402
7. Weidner N (1999) Tumour vascularity and proliferation: clear evidence of a close relationship. J Pathol 189(3):297–299
8. Vayrynen SA et al (2016) Clinical impact and network of determinants of tumour necrosis in colorectal cancer. Br J Cancer 114(12): 1334–1342
9. Eberhard A, Kahlert S, Goede V, Hemmerlein B, Plate KH, Augustin HG (2000) Heterogeneity of angiogenesis and blood vessel maturation in human tumors: implications for antiangiogenic tumor therapies. Cancer Res 60(5):1388–1393
10. Pollheimer MJ, Kornprat P, Lindtner RA, Harbaum L, Schlemmer A, Rehak P, Langner C (2010) Tumor necrosis is a new promising prognostic factor in colorectal cancer. Hum Pathol 41(12):1749–1757
11. Richards CH, Roxburgh CSD, Anderson JH, McKee RF, Foulis AK, Horgan PG, McMillan DC (2012) Prognostic value of tumour necrosis and host inflammatory responses in colorectal cancer. Br J Surg 99(2):287–294
12. Swinson DE et al (2002) Tumour necrosis is an independent prognostic marker in non-small cell lung cancer: correlation with biological variables. Lung Cancer 37(3):235–240
13. Pichler M, Hutterer GC, Chromecki TF, Jesche J, Kampel-Kettner K, Rehak P, Pummer K, Zigeuner R (2012) Histologic tumor necrosis is an independent prognostic indicator for clear cell and papillary renal cell carcinoma. Am J Clin Pathol 137(2):283–289
14. Loupakis F, Schirripa M, Caparello C, Funel N, Pollina L, Vasile E, Cremolini C, Salvatore L, Morvillo M, Antoniotti C, Marmorino F, Masi G, Falcone A (2013) Histopathologic evaluation of liver metastases from colorectal cancer in patients treated with FOLFOXIRI plus bevacizumab. Br J Cancer 108(12):2549–2556
15. Ishida K, Uesugi N, Hasegawa Y, Sugimoto R, Takahara T, Otsuka K, Nitta H, Kawasaki T, Wakabayashi G, Sugai T (2015) Proposal for novel histological findings of colorectal liver metastases with preoperative chemotherapy. Pathol Int 65(7):367–373
16. Wicherts DA, de Haas RJ, Sebagh M, Saenz Corrales E, Gorden DL, Lévi F, Paule B, Azoulay D, Castaing D, Adam R (2011) Impact of bevacizumab on functional recovery and histology of the liver after resection of colorectal metastases. Br J Surg 98(3): 399–407
17. Ng JK et al (2008) Colorectal liver metastases contract centripetally with a response to chemotherapy: a histomorphologic study. Cancer 112(2):362–371
18. Paget S (1989) The distribution of secondary growths in cancer of the breast. Cancer Metastasis Rev 8(2):98–101
19. McCrea KA, Ensor JE, Nall K, Bleecker ER, Hasday JD (1994) Altered cytokine regulation in the lungs of cigarette smokers. Am J Respir Crit Care Med 150(3):696–703
20. Kuschner WG, D'Alessandro A, Wong H, Blanc PD (1996) Dose-dependent cigarette smoking-related inflammatory responses in healthy adults. Eur Respir J 9(10):1989–1994
21. Hiratsuka S, Watanabe A, Aburatani H, Maru Y (2006) Tumour-mediated upregulation of chemoattractants and recruitment of myeloid cells predetermines lung metastasis. Nat Cell Biol 8(12): 1369–1375
22. Hiratsuka S, Watanabe A, Sakurai Y, Akashi-Takamura S, Ishibashi S, Miyake K, Shibuya M, Akira S, Aburatani H, Maru Y (2008) The S100A8-serum amyloid A3-TLR4 paracrine cascade establishes a pre-metastatic phase. Nat Cell Biol 10(11):1349–1355
23. Yahagi M, Tsuruta M, Hasegawa H, Okabayashi K, Toyoda N, Iwama N, Morita S, Kitagawa Y (2017) Smoking is a risk factor for pulmonary metastasis in colorectal cancer. Color Dis 19(9): O322–O328